CrossMark

Tri-Scan: A Three Stage Color Enhancement Tool for Endoscopic Images

Mohammad S. Imtiaz[1] · Shahed K. Mohammed[1] · Farah Deeba[1] · Khan A. Wahid[1]

Abstract Modern endoscopes play a significant role in diagnosing various gastrointestinal (GI) tract related diseases where the visual quality of endoscopic images helps improving the diagnosis. This article presents an image enhancement method for color endoscopic images that consists of three stages, and hence termed as "Tri-scan" enhancement: (1) tissue and surface enhancement: a modified linear unsharp masking is used to sharpen the surface and edges of tissue and vascular characteristics; (2) mucosa layer enhancement: an adaptive sigmoid function is employed on the R plane of the image to highlight micro-vessels of the superficial layers of the mucosa and submucosa; and (3) color tone enhancement: the pixels are uniformly distributed to create an enhanced color effect to highlight the subtle micro-vessels, mucosa and tissue characteristics. The proposed method is used on a large data set of low contrast color white light images (WLI). The results are compared with three existing enhancement techniques: Narrow Band Imaging (NBI), Fuji Intelligent Color Enhancement (FICE) and i-scan Technology. The focus value and color enhancement factor show that the enhancement level achieved in the processed images is higher compared to NBI, FICE and i-scan images.

Keywords Color image enhancement · Unsharp masking · Adaptive sigmoid function · Wireless capsule endoscopy

This article is part of the Topical Collection on *Systems-Level Quality Improvement*

✉ Khan A. Wahid
khan.wahid@usask.ca

1 Department of Electrical and Computer Engineering, University of Saskatchewan, S7N5A9, Saskatoon, SK, Canada

Introduction

Visual quality of a color image plays a significant role in the diagnosis of endoscopic images. Some gastrointestinal (GI) related diseases such as stomach and colon cancers and ulcerative colitis are now of significant threats to human's health. According to the statistics of Hong Kong Cancer Registry in 2007, the number of bowel cancer cases in Hong Kong ranked the second of all cancer cases, and it was approaching the highest [1]. Diagnosis of endoscopic images of the GI tract is routinely carried out by performing flexible wired endoscopy or wireless capsule endoscopy (WCE). Of the two, WCE is the recently established methodology that offers a noninvasive procedure [2]. However, due to power and hardware limitations, the image quality in WCE is lower than wired endoscopy [3]. Wired endoscopy often misses a significant amount of tissue and vascular characteristics leading to a delayed or suboptimal therapies through the misinterpretation of the findings. Additionally, endoscopic images suffer from various kinds of degradations resulted from inadequate illumination [3] and transmission error. The gastric organ has its own convolution, bending and waving natures, so the images inevitably suffer from inhomogeneous brightness and poor contrast. These degradations present challenges to computer-aided detection (CAD) because features of the disease might be too obscure for detection. The features of endoscopic images should be appropriately enhanced to facilitate the detection of diseases and also the development of efficient CAD algorithms, such as segmentation [4], tumor or lesion detection [5, 6] and bleeding detection [7].

There are two types of processing systems that may be used to enhance certain mucosal or vascular characteristics: in-chip and off-line. Two new in-chip technologies, providing the enhancement with in-chip processor, are known as narrow band imaging (NBI) [8] and auto-florescence imaging (AFI)

[9]. A number of filters with specific wavelengths are used in these technologies that eventually increase the hardware complexity and power consumption of the endoscopic system [9, 10]. Among off-line techniques that provide enhancement in post-processing stage, virtual chromoendoscopy (CE), also known as Fuji Intelligent Color Enhancement (FICE) [11], is often used that can simulate an infinite number of wavelengths in real time. Here, the software applies an algorithm to the real-time endoscopic image, which is reconstructed to determine a wavelength for each of the three colors (red, green, blue). The image is instantaneously reconstructed after changing the wavelengths with virtual electronic filters. There is another method, known as i-scan by PENTAX [12], which modifies pixel sharpness, hue and contrast in real-time. Studies showed that i-scan technology can improve the diagnostic accuracy [13]. In another tandem clinical trial, the authors showed that compared to the conventional WLI, i-scan can increase the detection rate of colorectal polyps and reduce the miss rate of adenomas [14]. Several researchers concluded that NBI appeared to be a less time-consuming and equally effective alternative to CE for the detection of neoplasia, but with higher miss rate [15, 16]. Additionally, neither NBI nor CE can improve the adenoma detection or reduce miss rates during screening colonoscopy. No difference has been observed in diagnostic efficacy between these two systems [17, 18].

Several recent works have exploited different image enhancement algorithms for improving the image quality of endoscopic images. For example, Okuhata et al. have presented a retinex based method, where they applied retinex theory to extract the true luminance of the image [19]. The resultant true luminance is gamma corrected to achieve higher contrast image. Beside contrast enhancement, several research efforts have been focused on denoising and deblurring. Gopi et al. proposed the use of double density dual-tree complex wavelet transform for colour image denoising [20]. A nonlinear technique known as Gaussianization transform is used in some works in literature where the probability distribution function (pdf) of an original image is converted to a Gaussian distribution so that their statistical properties can be calculated analytically and then enhanced separately. It is applied in [21] in combination with nonlinear statistical modeling to enhance retinal Optical Coherence Tomography (OCT) images. In another work [22], Gaussianization was also applied in the log-transform domain (also known as transform histogram shaping) to adjust the parameters to enhance the contrast of the image while preserving critical information. However, the application of these techniques to color images has not yet been explored and as they are limited to grayscale images only.

Most of these works focuses on contrast enhancement to increase mucosal illumination in endoscopy imaging [23]. Color tone is generally kept preserved in these methods. However, i-scan, NBI and FICE exploit the color tone

enhancement to extract unique features from the different spectral response. Similarly, image processing algorithms that can leverage the unique characteristics of different spectral response in the endoscopic image, can provide better enhancement in terms of better visualization of the anomaly in the image.

In this paper, a new color image enhancement scheme, termed as "tri-scan", is proposed. The process has three stages: tissue and surface enhancement (TSE), mucosal layer enhancement (MLE) and color tone enhancement (CTE). TSE is employed using modified linear unsharp masking (MLUM); MLE is performed in red (R) plane of the sharpened color image using adaptive sigmoid function. Finally, in CTE the pixels of three color planes are uniformly distributed to increase the contrast level and to create an enhanced color tone. As a whole it is shown that the proposed scheme can enhance the mucosa structures and tissue characteristics, and also highlight the micro-vessels of the superficial layers of the mucosa and sub-mucosa present in the endoscopic images.

Methodology

Our main goal is to tune endoscopic RGB images, often of obscure phosphor chromaticity, in a way that the subtle features become highlighted. The RGB planes carry different spectral responses of the surface [24]. These spectral responses are mainly dependent on the camera sensor and its spectral sensitivity. From the observation of spectral sensitivities ranging from 300 nm to 700 nm of CMOS and CCD cameras and their effect on endoscopic images, it can be noticed that R plane dominates higher wavelength, G plane dominates mid-wavelength, and B plane dominates shorter wavelength regions. As a result, these individual spectral responses of R, G and B planes carry different spatial characteristics. From Fig. 1, it is noticeable that the edges and lesion borders are only visible in G and B planes, mostly carrying the information related to the superficial layers of the mucosa structure.

On the other hand, the subtle blood vessels and micro-vessels located deeper in the mucosal layer are better visible in R plane, primarily carrying information related to deep mucosa layer than the other plane. In Fig. 1(a) and (b), the arrow sign indicates a blood vessel, which is more clearly visible in the R plane of the original color image. It is possible to highlight these subtle features by enhancing these different spatial characteristics separately. The proposed enhancement method works on each plane separately to highlight these subtle features to help the gastroenterologists to inspect the tissue characteristics, mucosa structures, and abnormal growths better than the original image.

The tri-scan scheme performs enhancement in each plane to highlight these subtle features of endoscopic images. It

Fig. 1 **a** Original RGB endoscopic image **b** R plane **c** G plane **d** B plane

(a)

(b)

(c)

(d)
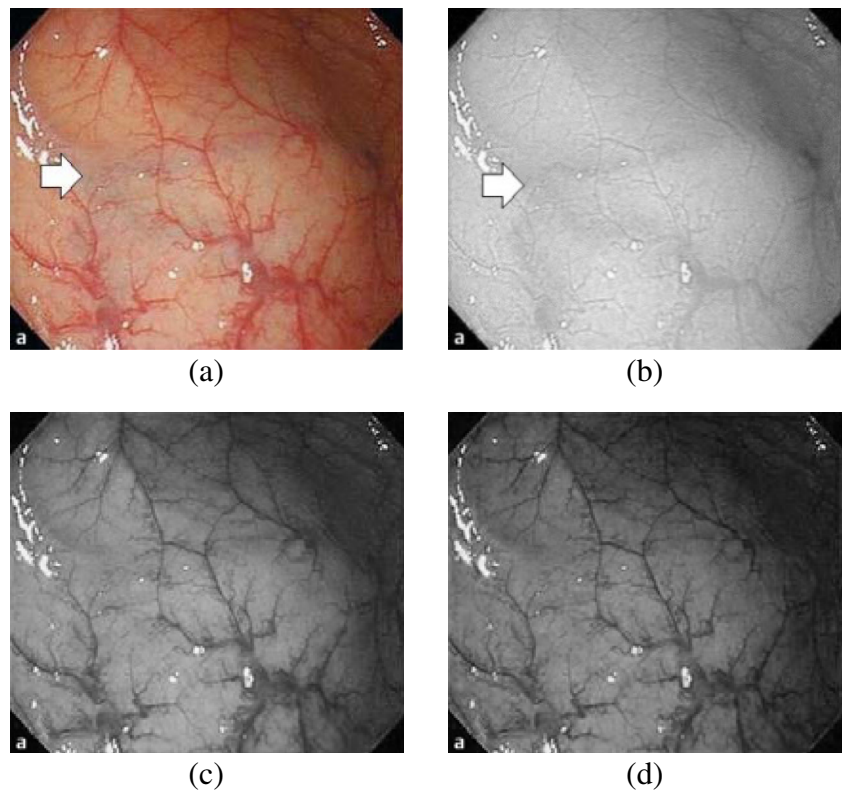
consists of three stages as shown in Fig. 2: tissue and surface enhancement (TSE), mucosal layer enhancement (MLE) and color tone enhancement (CTE). An illustration of the changes in spatial characteristics in each plane of the endoscopic image is shown in Fig. 3. The stages are discussed below:

Tissue and surface enhancement (TSE)

At first, the WLI endoscopic image is divided into three primary color planes: R, G, and B. These color planes are normalized between 0 and 1 using (1). In TSE stage, each of these color planes is treated as a grayscale image.

$$N(x) = \frac{x - x_{\min}}{x_{\max}} \tag{1}$$

Here, the mucosa structures, tissue and vascular characteristics, and pit patterns in each plane are enhanced using modified linear unsharp masking (MLUM). Traditionally, UM is a sharpening operator that can enhance edges and other high frequency components via a procedure that subtracts an unsharp or blurry version of an image from the original grayscale image [25]. It produces an edge image $g(x, y)$ from an input gray scale image $f(x, y)$ using (2).

$$g(x, y) = f(x, y) - f_{\text{blurry}}(x, y) \tag{2}$$

Where, $f_{blurry}(x, y)$ is the blurry version of $f(x, y)$. Here, a $3x3$ mean filter (shown in Fig. 4) is used to produce the blurry image from the original gray scale image. It is a simple sliding-window spatial filter that replaces the center value with a mean value of all pixels in the window.
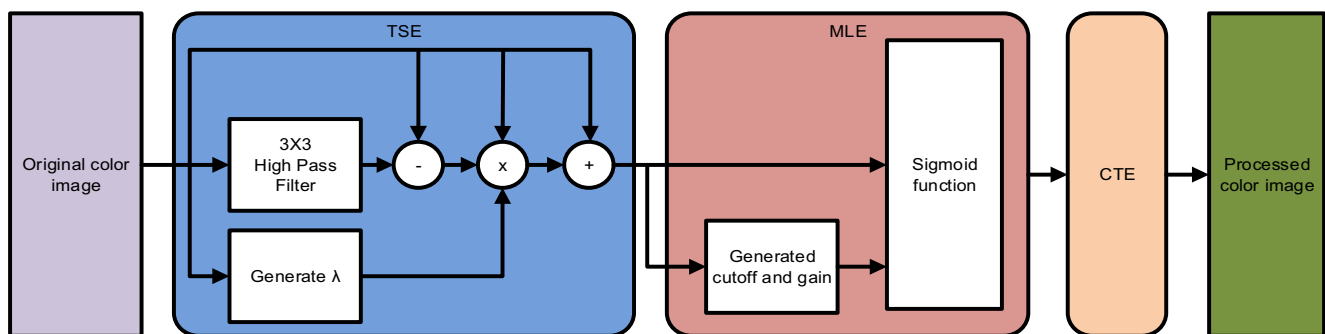
Fig. 2 Overview of Tri-scan scheme
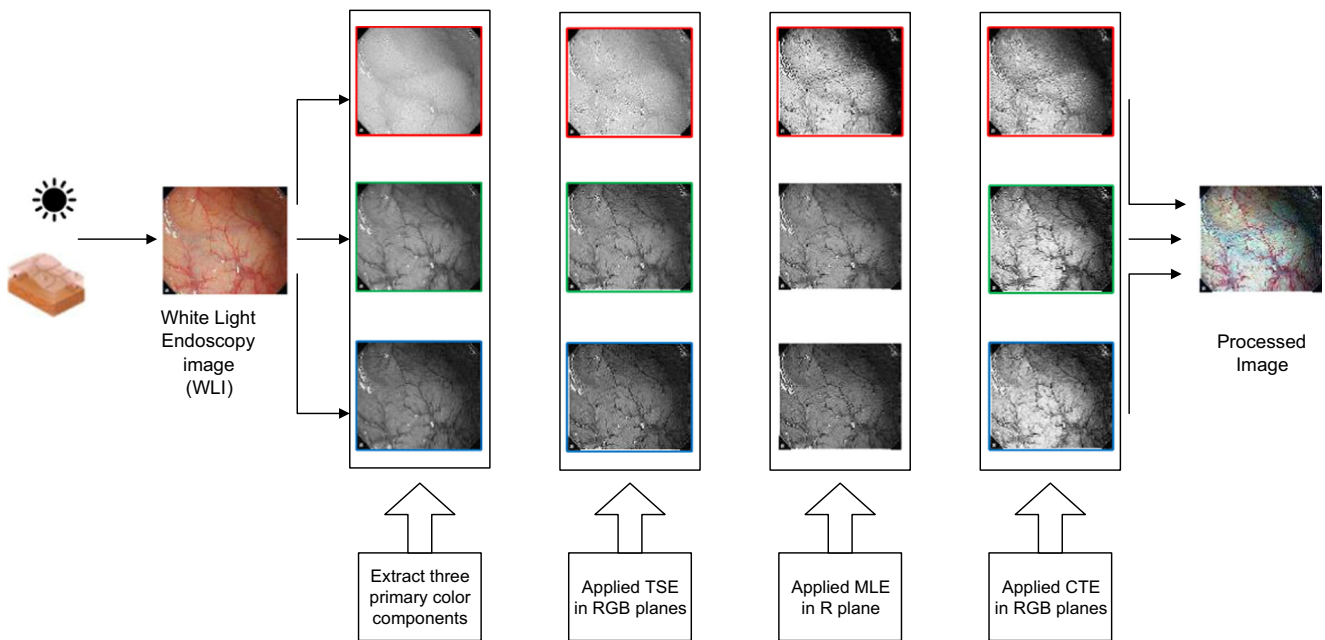
Fig. 3 A visual illustration of the changes in spatial characteristics in each plane of the endoscopic image using tri-scan method

The edge image carries all high frequency components of the original image. These high frequency components are intensified by multiplying a sharpening factor λ with the edge image. Finally, it is added to the original gray scale image $f(x, y)$ to produce the sharpened image using (3).

$$f_{sharpen}(x, y) = f(x, y) + \lambda \times g(x, y) \qquad (3)$$

Here, $f_{sharpen}(x, y)$ is the sharpened image. The higher the sharpening factor, the more the sharpened images. However, at a certain level, sharpening may introduce artificial artifacts that make the controlling of the sharpening factor based on the input pixels crucial. From the observation of R, G and B planes for different endoscopic images, it has been found that R planes has higher mean intensity than the G and B planes. Again, the edges and background in R plane has lower contrast while the G and B plane has higher contrast. To enhance the subtle characteristics, the sharpening factor must be higher for R plane. Smaller sharpening factor can provide sufficient contrast in G and B plane. From

these observations, we have proposed an algorithm to control the sharpening factor based on input pixel using (4). Here the sharpening factor is taken as proportional to the mean value to provide greater contrast in the R plane than G and B plane. The proportionality factor was taken from experiment for highest enhancement and highest structure similarity index. It keeps the sharpening factor in a certain range to provide maximum enhancement with little or no artificial information.

$$\lambda = 10 \times \frac{\sum_{i=1}^{n} f(x, y)}{n} \qquad (4)$$

Here, n is the number of pixels. At first, λ is generated from the input gray scale image $f(x, y)$ and used in (3) to generate the sharpened image.

Now, MLUM is employed in each plane of the color endoscopic image to sharpen the edges and borders of mucosa surfaces, pit patterns and tissue and vascular characteristics. From Fig. 5, we can see the changes of tissue characteristics and mucosa surface in the original, blurry and sharpened color images.

Mucosa layer enhancement (MLE)

In MLE stage, the superficial layers of mucosa, and size and pattern of micro-vessels are enhanced and highlighted using contrast manipulation techniques. Contrast manipulation technique can be employed either globally or adaptively. Global
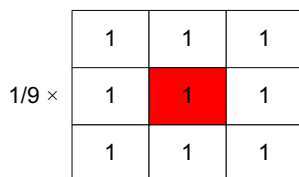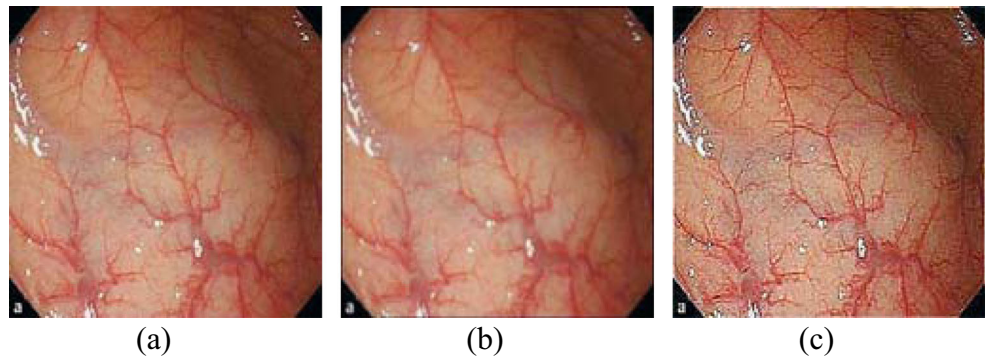

Fig. 4 3 × 3 mean filter

(a)   (b)   (c)

techniques apply same transformation to image pixels while adaptive techniques use an input-output transformation that varies adaptively with local image characteristics. Here, we have used an adaptive sigmoid function (ASF) to enhance mucosal layer information. As the R plane carries the spatial characteristics of superficial layers of mucosa, and size and pattern of microvessels (as previously mentioned), ASF is applied only on the R plane of the sharpened color image.

In general, a sigmoid function is real-valued and differentiable, have either a non-negative or non-positive bell shaped first derivative [26–28]. Using x for the input, the sigmoid function is given below:

$$S(x) = \frac{1}{(1 + e^{-x})} \qquad (5)$$

The limitation of (5) is the lack of versatility. To control the exponent, we have introduced two coefficients in the sigmoid function. Using x for the input, g for gain and k for cutoff, the modified sigmoid function is expressed below:

$$S(x) = \frac{1}{(1 + e^{g(k-x)})} \qquad (6)$$

The cutoff value determines the midpoint of the input curve, and the gain controls the amount of bending. These parameters (gain and cut-off) can also control the overall brightness and contrast level of the input image respectively. The cut-off value controls the amount of brightness, and the gain controls the consecutive difference between brightness. These two parameters give us the opportunity to control and train the proposed technique to generate a certain exponent that highlights the subtle features. Let, $x = 0, 0.1, 0.2, \dots, 1$ normalized image pixel values where the sigmoid function (6) is applied. Figure 6(a) shows the sigmoid curve of input pixel values based on different cut-off and gain, and the corresponding sigmoid images. Different combinations of gain and cut-off values generate different sigmoid images. In Fig. 6(b) and (d), we can observe the changes in superficial layers of the mucosa, which is previously mentioned in Fig. 1 using an arrow sign.

As mentioned before, R plane has higher brightness and lower contrast than the other two planes. To improve the image quality, the contrast should be increased, which in turn will reduce the brightness level. So, the cutoff value should be such that, it would be slightly less than the original mean value to reduce the brightness level. Again, if the mean intensity of the R plane is high, the gain value must be high to

Fig. 6 **a** Sigmoid function used in MLE stage; Sigmoid images with (**b**) gain = 14 gain, cutoff = 0.75; **c** gain 5, cutoff = 0.5; **d** gain = 12, cutoff = 0.7; **e** gain = 8 gain, cutoff =0.6

(a)   (b)   (c)

                                            (d)   (e)

Fig. 7 Processed endoscopic image at different stages of tri-scan algorithm

provide higher contrast. If the mean intensity of the R plane is low, the gain value must be low to avoid introducing artifacts. To maintain the exponent within the target range, we have proposed two algorithms to generate cut-off and gain values. Based on the input pixels, Eqs. (7) and (8) generate specific cut-off and gain values.

Fig. 8 Sample processed endoscopic images using tri-scan method

Later, these values are used in (6) to generate the sigmoid pixels for R plane.

$$k = z + \frac{1}{2}^* \left(\frac{\sum\limits_{i=1}^{n} x_i}{n} \right) \qquad (7)$$

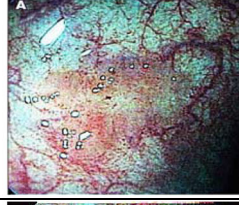$$g = \alpha \times \ln\left(\frac{\beta}{\sigma}\right) \times \frac{\sum\limits_{i=1}^{n} x_i}{n} \qquad (8)$$
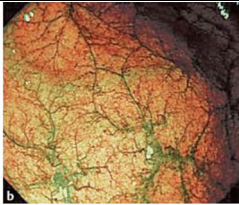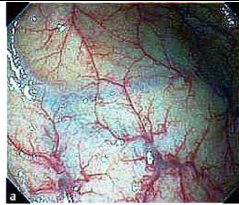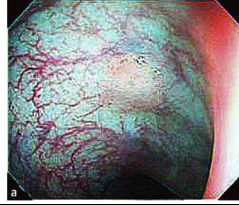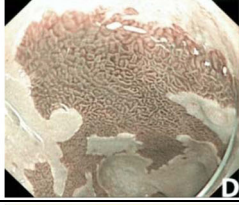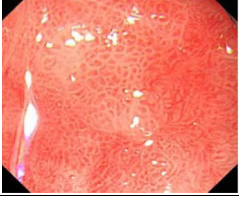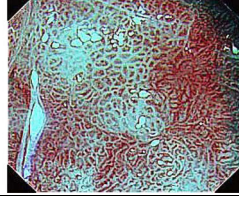
Where, $z = 0.2$, $\alpha = 10$, $\beta = 23$ and $\sigma = 10$, x_i is the input pixel values of ith position of R plane and n is the number of pixels. These values are heuristically collected from training mode such that maximum contrast is provided with minimum deviation in the structural similarity between the processed and original image. In Fig. 7, we can see the difference of R plane between the TSE and MLE stage. The superficial layers of the mucosa are better visible in the MLE stage compare to the TSE stage, which is more prominently evident in the color image at this stage.

Color tone enhancement (CTE)

In CTE stage, we have applied three-dimensional (3-D) uniform distributions to modify the pixels of R, G and B planes. The 3-D uniform distribution is accomplished by effectively spreading out the most frequent intensities. It eventually increases the contrast level and creates a pseudo color background, which provides a better visualization of mucosa structures, pit patterns, superficial layers 7and abnormal growths.

Fig. 9 Comparison between original raw endoscopic images, NBI images and Tri-scan images

Let, f is a given image represented as m by n matrix of integer pixel intensities of three dimension ranging from 0 to $L-1$. Let, p denotes the normalized values of f. Then,

$$P_n = \frac{\text{Number of pixels with intensity } n}{\text{total number of pixels}} \quad (9)$$

Where, $n = 0, 1, 2, \ldots, L-1$. It will generate P_n for all three dimensions.

The 3-D uniform distribution is expressed as:

$$\Psi_{r,g,b} = \begin{cases} \text{floor}\left((L_r-1)\sum_{n=0}^{fr_{i,j}} p_{rn}\right), & R\text{ plane} \\ \text{floor}\left((L_g-1)\sum_{n=0}^{fg_{i,j}} p_{gn}\right), & G\text{ plane} \\ \text{floor}\left((L_b-1)\sum_{n=0}^{fb_{i,j}} p_{bn}\right), & B\text{ plane} \end{cases} \quad (10)$$

Here, $floor()$ rounds the pixel value down to the nearest integer. In CTE, the 3-D uniform distribution of pixels of R,
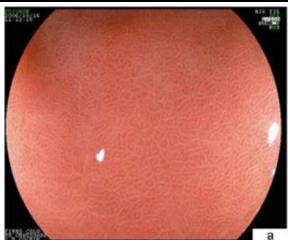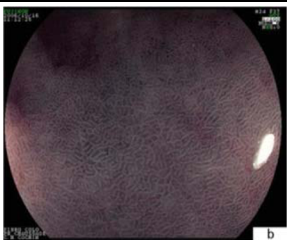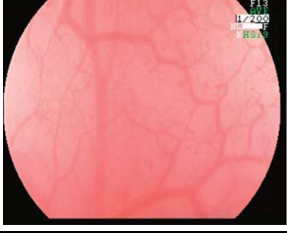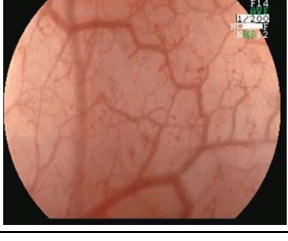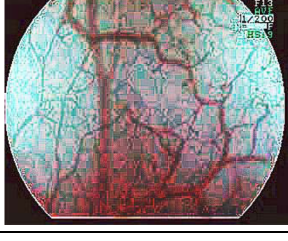

Fig. 10 Comparison between original raw endoscopic images, FICE images and Tri-scan images

G and B plane have been done by flatting the cumulative distribution function (CDF) using (9) and (10). The 3-D uniform distribution creates light steel blue effect on the overall endoscopic image, thus increases the visualization of the subtle mucosa structure, pit patterns, superficial layers, and abnormal growths. It also employs Indian red color effect on the tissue characteristics and mucosa structures, and royal blue effect on the superficial layer of mucosa. In Fig. 7 (CTE section), we can see the color effect on a typical endoscopic image.

Results and discussion

To evaluate the performance of tri-scan technology, we have applied it on several endoscopic images collected from Gastrolab [29], Atlas [30], FICE atlas [31] and i-scan mini atlas [12] databases. The results are summarized in the following categories:

Category 1: Low contrast color images

In this case, the tri-scan method is applied to several low contrast color endoscopic images. The results are presented in Fig. 8. Here, it is noticeable that the mucosa structures and tissue characteristics are more highlighted in the processed images in comparison to the original raw endoscopic images. The reason for enhancement is the application of MLUM to sharpen the edge and borders of the images. Furthermore, the application of ASF enhances and highlights the micro-vessels of the superficial layers of mucosa and sub-mucosa. The aggravation in the pattern and size of micro-vessels are

much more defined and discernible in the processed images. Additionally, tri-scan method creates light steel blue effect in the background, Indian red effect on the structures and royal blue effect on the subtle mucosa layer by using 3-D uniform distribution, which helps to distinguish the pit patterns and abnormalities in the mucosa structures and layers.

Category 2: Comparison with NBI

In the second experiment, tri-scan scheme is compared with NBI images. The results are presented in Fig. 9. Here, we can see the original raw endoscopic images and their corresponding NBI and tri-scan images. For NBI, the submucosal vessels are displayed in cyan color. As a result, the mucosal structures are displayed with greater contrast than in WLI. This is evident in Fig. 9 from the comparison of WLI and the corresponding NBI. However, with royal blue effect to the superficial mucosa layer and Indian red effect on the structure, the superficial blood vessel is easily distinguishable in the tri-scan image. For example, In Fig. 9 (1), a Y-shape blood vessel in the superficial layer of mucosa is easily visible in the processed image, but is not so discernible in the original and NBI image. In Fig. 9 (2) and (4), the water shaded surface and pit patterns are more clearly visible in the processed images. In Fig. 9 (3) and (5), the mucosa structures, size and pattern of micro-vessels in the processed images are more highlighted because of the light steel blue background effect.

Category 3: Comparison with FICE

For the next case, we compared tri-scan with FICE images. The results are presented in Fig. 10. It is seen that FICE can
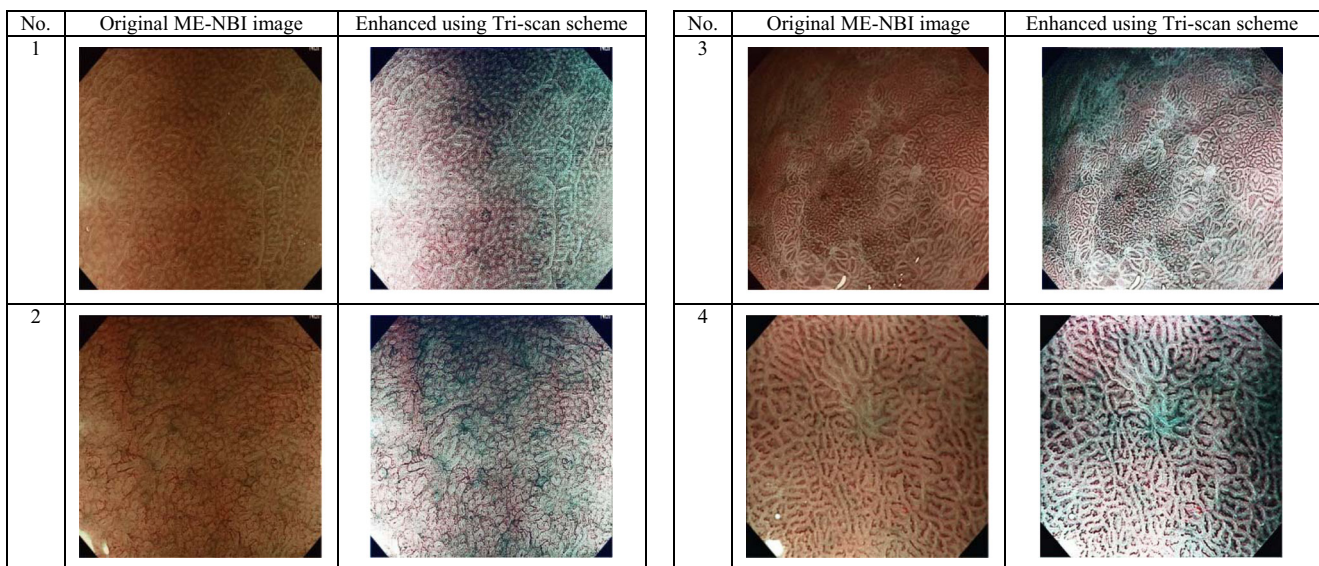
Fig. 11 Comparison between ME-NBI images and Tri-scan images

provide image with well-defined mucosal structure. But due to the CTE provided by the tri-scan scheme, more subtle characteristics are revealed. Also, it highlights the vascular characteristics better than FICE images, as shown in Fig. 10(1).

Category 4: Comparison with ME-NBI images
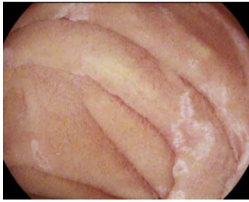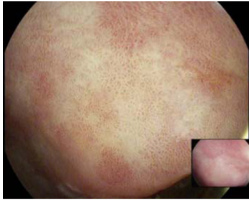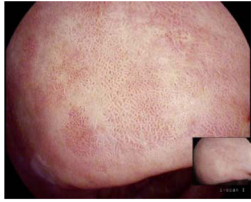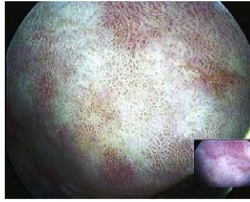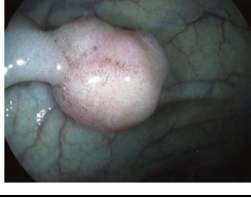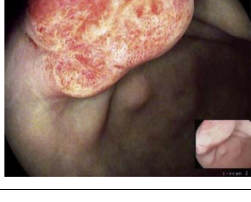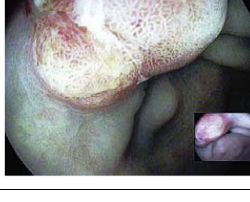
In this case, the tri-scan technique is employed on magnified endoscopic (ME) NBI images for further enhancement. The results are presented in Fig. 11. The mucosal structure, size and pattern of micro-vessels are better visible in the processed images compared to the ME-NBI images.

Category 5: Comparison with i-scan technology

PENTEX, Japan has developed a post processing technology, known as i-scan, for enhancing the endoscope image. The method is proprietary and the database is limited. As a result,

Fig. 12 Comparison between i-scan image and Tri-scan images

we have compared it with ours using the available images from Mini-Atlas [12]. The results are shown in Fig. 12. It is seen that the images enhanced by i-scan show some improved mucosal structure and lesion region while the proposed tri-scan scheme shows mucosal structure which is more detectable with the crisp edges. The lesion and bleeding regions are also well defined and distinguishable with the contrast provided by the color tone of the proposed method. It is also capable of enhancing subtle abnormalities that the i-scan method could not perform (see Fig. 12 (3) and (4)).

Category 6: Comparison with other methods

To evaluate the performance of the proposed method further, we have compared it with four other contrast enhancement methods. They are: Contrast limited adaptive histogram equalization (CLAHE) [32, 33], contrast stretching (CS) [34], high boost filtering (HBF) [34], and unsharp masking (UM) [35]. Visual comparison of these methods is shown in Fig. 13. The results are presented later in "Comparison with other methods" section.

Performance analysis

In following section, the performance of the tri-scan method is evaluated using the following parameters:

Focus value

In the proposed tri-scan method, the information on sharp counters, edges and contrast in an image is increased. These changes are evaluated using the ratio of AC and DC energy of

Table 1 Comparisons of focus value between NBI and Tri-scan

Image no.	Focus value		
	Original	NBI	Tri-scan
1	11.33	25.67	39.68
2	13.12	27.29	40.15
3	8.74	16.17	30.67
4	5.29	9.25	40.53
5	9.47	14.28	29.13
Avg. of 60 endoscopic images	17.63	20.71	38.78

a Discrete Cosine Transform (DCT) image, known as focus value [36, 37]. Let E_{AC} and E_{DC} are the energy of AC and DC components of the DCT image as given below:

$$E_{DC} = (F_{DC}(u,v))^2 \tag{11}$$

$$E_{AC} = \sum_{u=1}^{n} \sum_{v=1}^{m} \left(F_{AC}(u,v) - \overline{F_{AC}(u,v)} \right)^2 \tag{12}$$

Here, u and v represent the row and column of the DCT image, F_{DC} is the DC part and F_{AC} is the AC part of DCT image. The resultant of the ratio of E_{AC} and E_{DC} is the focus value F_S as given by Eq. (13):

$$F_S = \frac{E_{AC}}{E_{DC}} \tag{13}$$

If the overall information of sharp counters, crisp edges and contrast of enhanced image is higher than the original image,
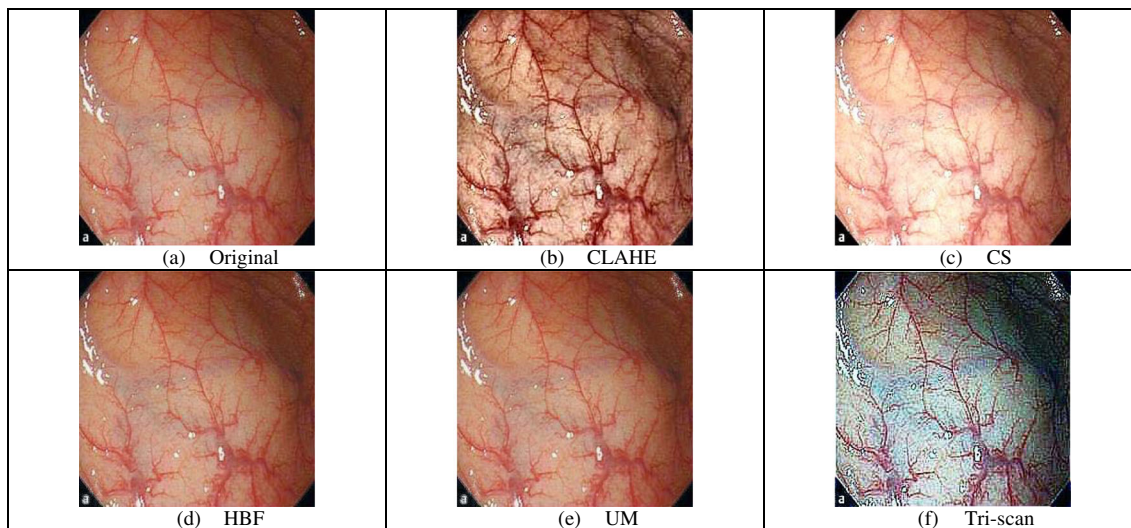
Fig. 13 Comparison with other contrast enhancement methods

Table 2   Comparisons of focus value between FICE and Tri-scan

Image no.	Focus value		
	Original	FICE	Tri-scan
1	26.84	22.36	39.18
2	26.68	35.06	43.89
3	34.12	55.81	66.98
4	33.49	38.06	46.01
5	33.29	37.47	41.28
Avg. of 60 endoscopic images	28.71	36.49	45.11

F_S will be higher than that of the original image and vice versa. We have compared tri-scan scheme in terms of focus value using 60 sample images with other methods such as, NBI [8] and FICE [31]. We have also compared with i-scan [12] in terms of focus value using eight sample images. The results are presented in Tables 1, 2 and 3. Here, we can observe that the focus values of all enhancement schemes are higher than the original image. Among the processing schemes, the focus value of tri-scan is the highest which indicates that tri-scan enhances different spectral characteristics separately.

## Statistic of visual representation

Next, we used the statistic of visual representation [38] to measure the contrast and intensity distortion between two images. Equations (14) and (15) represent statistic visual representation.

$$C = \frac{\sigma_{out} - \sigma_{in}}{\sigma_{in}} \quad (14)$$

Table 3   Comparisons of focus value between i-scan and Tri-scan

Image no.	Focus value		
	Original	i-scan	Tri-scan
1	16.06	25.41	57.31
2	33.67	76.87	58.90
3	15.89	27.93	59.29
4	26.43	46.55	58.74
5	51.21	43.96	58.71
6	28.95	47.29	59.62
7	30.02	52.63	59.32
8	27.60	31.93	60.13
Avg. of eight endoscopic images	28.73	44.07	59.00

Table 4   Comparisons of statistic of visual representation between NBI and Tri-scan

Image no.	Contrast measurement		Intensity measurement	
	NBI	Tri-scan	NBI	Tri-scan
1	1.2480	1.7597	−0.0169	0.0699
2	1.2076	1.8823	−0.0782	0.0516
3	1.2163	1.6856	−0.0931	0.3054
4	2.0255	2.8647	−0.0122	0.0092
5	1.1697	1.7294	−0.2234	0.1649
Avg. of 60 endoscopic images	1.4253	1.9381	−0.0549	0.0901

$$L = \frac{L_{out} - L_{in}}{L_{in}} \quad (15)$$

Where, σ_{out} and L_{out} are the σout variance and mean of the enhanced image; σ in and L_{in} are the variance and mean of the original image, respectively. Here, C defines the percentage of increment or decrement of contrast level and L defines the percentage of increment or decrement in intensity level. In our experiment, we have compared tri-scan in terms of statistic of visual representation using 60 sample images with other methods like NBI [8] and FICE [31]. We have also compared the proposed method with i-scan [12] using eight sample images. The results are presented in Tables 4, 5 and 6. We can see that the C and L of the first image using proposed method are 1.7597 and 0.0699, which means the contrast and intensity level of proposed image are 175.97 and 6.99 times higher than the original image respectively. Here, the negative sign denotes the decrement. It is noticeable that the contrast

Table 5   Comparisons of statistic of visual representation between FICE and Tri-scan

Image no.	Contrast measurement		Intensity measurement	
	FICE	Tri-scan	FICE	Tri-scan
1	0.9876	1.5460	−0.4818	0.0680
2	1.0422	1.6565	−0.0511	0.0217
3	0.9411	1.1160	−0.1985	0.0105
4	0.7020	1.4578	−0.0933	0.0161
5	0.6216	1.5192	−0.1974	0.1428
Avg. of 60 endoscopic images	0.7947	1.5016	−0.1958	0.0819

Table 6 Comparisons of statistic of visual representation between i-scan and Tri-scan

Image no.	Contrast measurement		Intensity measurement	
	i-scan	Tri-scan	i-scan	Tri-scan
1	−0.1334	1.2772	−0.2294	−0.0750
2	−0.0633	0.5562	−0.5516	0.0013
3	−0.0102	1.3108	−0.3730	−0.1963
4	0.2228	0.7551	−0.1779	−0.0047
5	0.1556	0.3945	−0.2791	0.2819
6	−0.0106	0.7862	−0.3662	−0.0691
7	0.2812	0.6756	−0.2222	0.0019
8	−0.2637	0.8829	−0.3273	−0.0910
Avg. of 8 endoscopic images	0.0233	0.8298	−0.3158	−0.0188

and intensity levels for images produced by Tri-scan are higher compared to that of other methods.

Color enhancement factor (CEF)

Next, we have evaluated our scheme in terms of color enhancement using a no-reference performance metric, called colorfulness metric (CM) [39]. CM measurement is based on the mean and standard deviations of two axes opponent color representation with, $\alpha = R - G$ and $\beta = \frac{1}{2}(R + G) - B$. The metric is defined as:

$$CM = \sqrt{\sigma_\alpha^2 + \sigma_\beta^2} + 0.3\sqrt{\mu_\alpha^2 + \mu_\beta^2} \qquad (16)$$

Where, σ_α and σ_β are standard deviations of α and β, respectively. Similarly, μ_α and μ_β are their means. However,

Table 7 Comparisons of CEF between NBI and Tri-scan

Image no.	CEF	
	NBI	Tri-scan
1	1.1998	1.5478
2	1.0453	1.4633
3	1.0072	1.7076
4	1.0584	1.5716
5	1.2725	1.6453
Avg. of 60 endoscopic images	1.2214	1.5119

Table 8 Comparisons of CEF between FICE and Tri-scan

Image no.	CEF	
	FICE	Tri-scan
1	1.1733	1.4716
2	1.3464	1.4788
3	1.4325	1.5010
4	1.3788	1.7222
5	1.3747	1.7244
Avg. of 60 endoscopic images	1.2711	1.5549

in our comparison, we have used the ratio of CMs between the enhanced and original image for observing the color enhancement factor (CEF). If $CEF < 1$, the original image is better compared to the enhanced image in terms of color image enhancement. CEF with value 1 indicates that there is no difference between the enhanced and original image in terms of color enhancement. We have compared our method in terms of CEF using 60 sample images with other methods like NBI [8] and FICE [28]. We have also compared our method with i-scan [12] using eight sample images. The results have been presented in Table 7, 8 and 9. Here, we can notice that CEF values of the proposed method are higher compared to other enhancement methods which indicate that our scheme performs better in terms of color enhancement.

Comparison with other methods

In Table 10, we compare our results with several other enhancement methods using 60 images taken from Endoscopic image database [29]. It is seen from the table that, Tri-scan produces better results in terms of CEF, focus value, contrast

Table 9 Comparisons of CEF between i-Scan and Tri-scan

Image no.	CEF	
	i-Scan	Tri-scan
1	1.79	2.26
2	2.24	2.19
3	2.47	2.52
4	2.33	2.01
5	2.48	2.53
6	2.33	3.39
7	2.87	2.28
8	3.01	3.87
Avg. of 8 endoscopic images	2.43	2.63

Table 10 Comparison of performance with other methods

Methods	CEF	Focus value	Contrast meas.	Intensity meas.	Comp. time (sec)
CLAHE [31, 32]	1.7877	7.1117	0.1938	0.0913	0.0865
CS [33]	1.9204	30.1941	0.5204	0.1683	0.0681
HBF [33]	1.7314	2.6697	−0.0228	0.0081	0.0234
UM [34]	1.7448	4.5629	0.0190	0.0003	0.1307
Tri-scan	1.9511	47.5026	0.5394	0.1723	0.1940

measurement and intensity measurement compared with other methods. The computational time is also reported in Table 10. All these algorithms were implemented using MATLAB R.2016 on a PC having Intel (R) Core (TM) i5-4210H CPU @ 2.90GHz and 8 GB of RAM. It is seen that, due to three step processing, Tri-scan consumes higher computational time than others. However, since all colour enhancement methods are meant for offline processing, the delay is insignificant. Besides, in a capsule endoscopy diagnosis, the system works at a frame rate of 2–4 frames per second; hence, Tri-scan can also be implemented for real-time color enhancement.

Subjective evaluation by physicians

In order to assess the quality of the enhanced images, we have conducted a small survey among several professional gastroenterologists. In the survey, four images were given to the observer: one original image and three processed image enhanced with TSE, TSE + MLE and TSE + MLE + CTE respectively; the observer was asked to rate the processed images based on the visibility of mucosa layer and neoplasm structure. There were three sets of images for each observer. The survey results are summarized in Table 11. Mean observer score (MOS) is used as the tool to interpret the results [40]. It is seen that, in all cases (except two), the processed images were rated as either highly or moderately enhanced. None of the processed images was marked for any distortion. This is

consistent with our claim using statistical metrics and indicates that the proposed Tri-scan algorithm is able to highlight the mucosa structures and neoplasm in endoscopic color images. Although the survey is short and provides positive and encouraging results, it does not have any clinical impact. We acknowledge that more exhaustive clinical trials with statistical tools such as the receiver operating characteristic [41] are needed to draw a final conclusion. This is however beyond the scope of this current work.

Conclusion

In this paper, we have presented a new color image enhancement method, named as tri-scan, for endoscopic images. The work focuses on enhancing the subtle features, which are not clearly visible in the original raw endoscopic images. It is achieved using enhancements on three different layers. The method highlights pit patterns, tissue and vascular characteristics in the endoscopic images and distinguishes them with different pseudo colors. It also highlights micro-vessels of the superficial layers of the mucosa and sub-mucosa, creating a light steel blue effect in the background, an Indian red effect on the mucosa structures and royal blue effect on the subtle mucosa layers. As a result, the mucosal structures become more visible when compared to the original raw endoscopic images.

Table 11 Survey results

Method	TSE			TSE + MLE			TSE + MLE + CTE		
Image #	Im1	Im2	Im3	Im1	Im2	Im3	Im1	Im2	Im3
Observer 1	1	1	2	1	1	2	1	1	2
Observer 2	2	2	1	1	1	1	0	1	0
Observer 3	2	2	1	2	2	1	1	2	1
MOS	1.67	1.67	1.33	1.33	1.33	1.33	0.67	1.33	1.00
Average MOS	1.56			1.33			1.00		

Highly enhanced = 2, moderately enhanced = 1, not enhanced at all = 0, moderately distorted = −1, highly distorted = −2 Im1 = imgae 1; Im2 = imgae 2; Im3 = imgae 3;

References

1. Li, B., and Meng, M.Q.-H., Wireless capsule endoscopy images enhancement via adaptive contrast diffusion. *J. Vis. Commun. Image Represent.* 23(1):222–228, Jan. 2012.

2. Brownsey, A., and Michalek, J., Wireless capsule endoscopy, *Am. Soc. Gastrointest. Endosc.*, 2010.

3. Brownsey, A., and Michalek, J., High definition scopes, narrow band imaging, chromoendoscopy, *Am. Soc. Gastrointest. Endosc.*, 2011.

4. Yousefi-Banaem, H., Rabbani, H., and Adibi, P., Barrett's mucosa segmentation in endoscopic images using a hybrid method: Spatial fuzzy c-mean and level set. *J. Med. Signals Sensors.* 6(4):231, 2016.

5. Karkanis, S.A., et al., Computer-aided tumor detection in endoscopic video using color wavelet features. *IEEE Trans. Inf. Technol. Biomed.* 7(3):141–152, 2003.

6. Deeba, F., et al., Efficacy evaluation of save for the diagnosis of superficial neoplastic lesion. IEEE Journal of Translational Engineering in Health and Medicine (2017). doi:10.1109/JTEHM.2017.2691339.

7. Sainju, S., Bui, F., and Wahid, K., Automated bleeding detection in capsule endoscopy videos using statistical features and region growing. *J. Med. Syst.* Springer, 38(4):25, 2014.

8. Machida, H., Sano, Y., Hamamoto, Y., Muto, M., Kozu, T., Tajiri, H., and Yoshida, S., Narrow-band imaging in the diagnosis of colorectal mucosal lesions: A pilot study. *Endoscopy.* 36: 1094–1098, 2004.

9. Schmitz-valckenberg, S., Holz, F.G., Bird, A.C., and Spaide, R.F., Fundus autofluorescence imaging: Review and perspectives. *Retina.* 28(3):385–409, 2008.

10. Kaltenbach, T., Sano, Y., Friedland, S., and Soetikno, R., American gastroenterological association (AGA) institute technology assessment on image-enhanced endoscopy. *Gastroenterology.* 134:327–340, 2008.

11. Kodashima, S., and Fujishiro, M., Novel image-enhanced endoscopy with i-scan technology. *World J. Gastroenterol: WJG.* 16(9): 1043, 2010.

12. *PENTAX Medical i-scan Mini- Atlas for Gastroenterology.* 2015 [online]. Available: http://www.pentaxmedical.de/media/c770769bdd45ff6481dcd60381870872/PENTAX_i-scan_Mini-Atlas.pdf

13. Nishimura, J., Nishikawa, J., Nakamura, M., Goto, A., Hamabe, K., Hashimoto, S., and Sakaida, I., Efficacy of i-Scan imaging for the detection and diagnosis of early gastric carcinomas. *Gastroenterol. Res. Pract.*, 2014. doi:10.1155/2014/819395.

14. Hoffman, A., Loth, L., Rey, J.W., Rahman, F., Goetz, M., Hansen, T., and Kiesslich, R., High definition plus colonoscopy combined with i-scan tone enhancement vs. high definition colonoscopy for

colorectal neoplasia: A randomized trial. *Dig. Liver Dis.* 46(11): 991–996, 2014.

15. Pohl, J., May, A., et al., Computed virtual chromoendoscopy: A new tool for enhancing tissue surface structures. *Thieme E-Journals - Endoscopy.* 39(1):80–83, Jan. 2007.

16. Chiu, H., Chang, C., et al., A prospective comparative study of narrow-band imaging, chromoendoscopy, and conventional colonoscopy in the diagnosis of colorectal neoplasia. *GUT Int. J. Gastroenterol. Hematol.* 56(3):373, 2007.

17. Curvers, W., et al., Chromoendoscopy and narrow-band imaging compared with high-resolution magnification endoscopy in Barrett's esophagus. *Elsevier - Gastroenterology.* 134(3): 670–679, 2008.

18. Chung, S.J., Kim, D., et al., Comparison of detection and miss rates of narrow band imaging, flexible spectral imaging chromoendoscopy and white light at screening colonoscopy: A randomised controlled back-to-back study. *Gut.* 63:785–791, 2014.

19. Okuhata, H., Nakamura, H., Hara, S., Tsutsui, H. and Onoye T., Application of the real-time Retinex image enhancement for endoscopic images. Proc. Engineering in Medicine and Biology Society (EMBC), 35th Annual International Conference of the IEEE, 3407–3410, 2013. doi:10.1109/EMBC.2013.6610273.

20. Gopi, V.P., and Palanisamy, P., Capsule endoscopic image denoising based on double density dual tree complex wavelet transform. *Int. J. Imag. Robot.* 9:48–60, 2013.

21. Agaian, S.S., Silver, B., and Panetta, K.A., Transform coefficient histogram-based image enhancement algorithms using contrast entropy. *in IEEE Trans. Image Process.* 16(3):741–758, March 2007.

22. Amini, Z., and Rabbani, H., Statistical modeling of retinal optical coherence tomography. *in IEEE Trans. Med. Imaging.* 35(6):1544–1554, June 2016.

23. Imai, F. H. and Berns, R. S., Spectral estimation using trichromatic digital cameras. *Proceedings of the International Symposium on Multispectral Imaging and Color Reproduction for Digital Archives,* Chiba University Chiba, Japan, 42:1–8, 1999.

24. Luft, T., Colditz, C. and Deussen, O., *Image enhancement by unsharp masking the depth buffer.* ACM, 2006.

25. Plaza, A., Benediktsson, J.A., Boardman, J.W., Brazile, J., Bruzzone, L., Camps-Valls, G., Chanussot, J., Fauvel, M., Gamba, P., and Gualtieri, A., Recent advances in techniques for hyperspectralimage processing. *Remote Sens. Environ.* 113:S110–S122, 2009.

26. Hassan, N., and Akamatsu, N., A new approach for contrast enhancement using sigmoid function. *The Int. J. of Arab Jour.* 1(2): 221–225, 2004.

27. Saruchi, Adaptive sigmoid function to enhance low contrast images. *Int. J. of Comp. App.* 55(4):45–49, 2012.

28. *Gastrolab – the gastrointestinal site.* 1996 [online]. Available: http://www.gastrolab.net/index.htm.

29. *Atlas of Gastrointestinal Endoscopy.* 1996 [online]. Available: http://www.endoatlas.com/index.html.

30. *FICE Atlas of Spectral Endoscopic images.* 2008 [online]. Available: http://www.fujinonla.com/inc/class/descargar.php?url=/archivos/catalogos/fice-atlas-esp.pdf.

31. Pizer, S.M., et al., Adaptive histogram equalization and its variations. *Comput. Vision, Graphics, Image Process.* 39:355–368, 1987.

32. Wang, Z., and Bovik, A.C., A universal image quality index. *Signal Processing Lett., IEEE.* 9:81–84, 2002.

33. Srivastava, R., Gupta, J.R.P., Parthasarthy, H., and Srivastava, S., PDF based unsharp masking, crispening and high boost filtering of digital images. *Commun. Comput. Informat. Sci.* 40:8–13, 2009.

34. Polesel, A., Ramponi, G., and Mathews, V.J., Image enhancement via adaptive unsharp masking. *IEEE Trans. Image Process.* 9:505–510, 2000.

35. Xu, X., Wang, Y., Tang, J., Zhang, X., Liu, X., et al. *Sensors.* 11(9): 8281–8294, 2011.

36. Shen, C. H., Chen, H.H., Robust focus measure for low-contrast images, *Consumer Electronics, 2006. ICCE'06. 2006 Digest of Technical Papers. International Conference on*, IEEE, pp. 69–70, 2006.

37. Balas, B., Nakano, L., and Rosenholtz, R., A summary-statistic representation in peripheral vision explains visual crowding. *J. Vis.* 9(12):1–18, Nov. 2009.

38. Pezzoli, A., et al., Interobserver agreement in describing video capsule endoscopy findings: A multicentre prospective study. *Dig. Liver Dis.* 43:126–131, 2011.

39. Fawcett, T., An introduction to ROC analysis. *Pattern Recogn. Lett.* 27:861–874, 2006.

40. Susstrunk, S. E., and Winkler, S., Color image quality on the internet. *Intern. Soc. Opt. Photn.*, pp. 118–131, 2003.

41. Iakovidis, D.K., and Koulaouzidis, A., Software for enhanced video capsule endoscopy: Challenges for essential progress. *Nat. Rev. Gastroenterol. Hepatol.* 12(3):172–186, 2015.